

pubs.acs.org/acsapm Article

# Intermolecular Hydrogen Bonding between Poly[(R)-3-hydroxybutyrate] (PHB) and Pseudoboehmite and Its Effect on Crystallization of PHB

Changhao Liu, Meng Jia, Jing Qu, Isao Noda, D. Bruce Chase, Reva Street, and John F. Rabolt\*



Cite This: ACS Appl. Polym. Mater. 2020, 2, 4762-4769



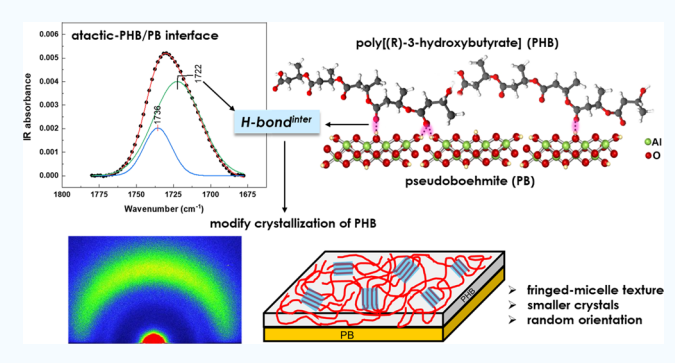
**ACCESS** 

III Metrics & More

Article Recommendations

s) Supporting Information

ABSTRACT: In the present study, we focused on the intermolecular H-bonding interactions of poly[(R)-3-hydroxybutyrate] (PHB) with an inorganic material, pseudoboehmite (PB), and their effect on PHB crystallization. Noncrystallizable atactic PHB and crystallizable isotactic PHB (a-PHB and i-PHB) ultrathin films were spin-coated on a PB substrate, as well as an aluminum oxide (AO) and a gold substrate for comparison. Infrared reflection—absorption spectroscopy (IRRAS) data show an absorption peak in the carbonyl region located at 1724 cm<sup>-1</sup> for a 2.8 nm a-PHB film deposited on PB. A peak at this frequency, often observed for thick bulk crystalline i-PHB films, was not observed for a 1.4 nm a-PHB film deposited on a gold or AO



substrate, indicating that the 1724 cm<sup>-1</sup> peak observed for a-PHB on PB is not due to a geometric confinement effect or crystallization but due to the existence of intermolecular H-bonding (H-bond<sup>inter</sup>) between -C=O of a-PHB and -OH from PB. Supercooled, amorphous i-PHB was also found to exhibit the same H-bond<sup>inter</sup> with PB. It was found that a PB surface significantly modified the crystal orientation and morphologies of the films. Grazing incident wide-angle X-ray diffraction (GIWAXD) data show that the crystallites in i-PHB on PB are randomly oriented, whereas those on AO are predominantly edge-on oriented. Polarized optical microscopy (POM) images show spherulites for i-PHB on AO, whereas no spherulites were observed for i-PHB on PB. This study demonstrates a novel method of using PB to modulate the crystallization behavior of PHB thin films.

KEYWORDS: poly[(R)-3-hydroxybutyrate] (PHB), pseudoboehmite (PB), crystallization, morphology, IRRAS, ultrathin films, confinement, H-bonding

# ■ INTRODUCTION

Poly[(R)-3-hydroxybutyrate], or PHB, is the most abundant polyester in the family of polyhydroxyalkanoates (PHAs) that are naturally made biodegradable aliphatic polyesters. 1,2 PHB serves as a carbon- and energy-storage material, produced in vivo in microorganisms. It has recently drawn considerable public attention because of its superior biodegradability and an urgent need to replace petroleum-based nondegradable polymers, such as polypropylene and polyethylene. The thermodynamically stable crystalline phase of PHB is the  $\alpha$ phase, which has an orthorhombic unit cell with the space group  $P2_12_12_1$  (a = 5.76 Å, b = 13.20 Å, and c = 5.96 Å).<sup>3,4</sup> A cooperative intramolecular hydrogen-bonding network (-C=O···H-C) was found in the  $\alpha$  crystalline structure. <sup>5,6</sup> PHB in bulk typically suffers from an excessively high crystallinity because of  $\alpha$  crystallization, which typically leads to high stiffness and brittleness.

Recently, substantial attention has been given to the study of PHB ultrathin films.<sup>7–13</sup> It was found that the crystallization behavior of PHB in ultrathin films deviates substantially from the bulk. Factors including spatial confinement, crystallization

temperature, substrate effect, and so forth could influence various aspects of crystallization, including crystallinity, crystal orientation, and morphology. In a sandwiched thin-film system, where PHB is the middle layer, inhibition of crystallization of PHB has been widely reported.<sup>7,8</sup> In these cases, spatial confinement is believed to be the key factor causing crystallization inhibition. In a one-free-surface film system, different crystallization behaviors were also observed. Khasanah *et al.* found that an intermediate crystalline state of PHB exists for a PHB ultrathin film crystallizing on a gold surface.<sup>9</sup> Sun *et al.* found that on a PVPh substrate, after melting, PHB stays in the amorphous state when the film is thinner than 175 nm,<sup>10</sup> which is attributed to interdiffusion of

Received: July 14, 2020 Accepted: August 31, 2020 Published: August 31, 2020





PHB with the PVPh sublayer. In another study by Sun *et al.*, <sup>11</sup> it was found that the thickness ratio of PHB and the PVPh sublayer plays a critical role in inducing different crystal morphologies for PHB.

Previously, we studied the surprising effect of an aluminum oxide (AO) substrate on the crystallization behavior of PHB and PHBHx. 14 We found that crystallization for a 40 nm PHB film was significantly retarded on the AO substrate. In the current study, we explore the crystallization behavior of PHB on the surface of pseudoboehmite (PB) or aluminum oxide hydroxide. Recently, PB was found to be capable of forming H bonds with ester-group-containing small organic molecules such as glycol di-(monomethyl succinic acid) ester, dimethyl adipate, and methyl oleate. 15,16 Such a H-bonding was shown to have a formation enthalpy of 19.8 kJ/mol, which is comparable to the crystallization enthalpy (12.5 kJ/mol) of i-PHB.6 H bonds formed between PHB, its copolymers, and other materials including cellulose acetate butyrate, 17 silica, 18 and poly(4-vinylphenol)<sup>19</sup> have also been demonstrated to significantly modify the crystallization behavior of polymers. In addition, it is found that PHB copolymers such as PHBV can form a H bond with the hydroxy groups in cellulose nanocrystal citrates, resulting in improved tensile strength, thermal stability, and water vapor barrier properties.<sup>20</sup>

In the present study, we focused on PHB ultrathin films deposited on a PB surface. To our knowledge, no study has been conducted to investigate the interaction between PB with polyesters such as PHB. We investigated the intermolecular interaction between PHB and PB. Infrared reflectionabsorption spectroscopy (IRRAS) was used for the H-bonding study with a particular focus on wavenumber shifts of the carbonyl stretching mode. We first examine intermolecular Hbonding interactions (or H-bond<sup>inter</sup>) of noncrystallizable atactic PHB (or a-PHB) with PB. An immersing study is used to determine the absorption frequency in the carbonyl region resulting from the H-bond<sup>inter</sup>. AO and gold substrates are used to eliminate the possibility of confinement effects causing the frequency shift. We also examine the effect of PB on melt crystallization of i-PHB using IRRAS, grazing incident wide-angle X-ray diffraction (GIWAXD), and polarized optical microscopy (POM).

# **■ EXPERIMENTAL SECTION**

**Materials.** Bacteria-synthesized isotactic PHB with a weight-averaged molecular weight  $(M_{\rm w})$  of \$40,000 g/mol was purchased from Sigma-Aldrich Inc (St. Louis, MO, US). Synthetic atactic PHB  $(M_{\rm w} \sim 169,000~{\rm g/mol})$  was supplied by the Procter & Gamble Company (Cincinnati, OH, USA). Chloroform was purchased from Fisher Scientific, while aluminum substrates were obtained from DRL Inc. Aluminum substrates were prepared by depositing aluminum onto a glass slide using physical vapor deposition. After deposition, aluminum was allowed to oxidize naturally at room temperature. The resulting deposited aluminum layer was approximately 100 nm thick with a 5 nm oxide layer as measured by transmission electron microscopy reported previously. The surface roughness (RMS) was determined to be 1.52 nm using a Dimension 3100 atomic force microscope.

**Preparation of Pseudoboehmite Substrates and PHB Ultrathin Films.** Preparation of PB substrates followed the method reported by van den Brand  $et\ al.^{21}$  A cleaned aluminum substrate was treated by immersing it into boiling, deionized water at 100 °C for 1 min. The substrate was then rapidly taken out of the water, and the residue was removed by flowing nitrogen across the surface. Then, the substrate was purged under nitrogen for another 30 min before spincoating.

For spin-coating, a solution of 0.5 wt % i-PHB in chloroform and 0.3 wt % a-PHB in chloroform was used. A total of 0.5 ml of solution and 1300 rpm/s acceleration rate were used. A spin-coating time of 3 min at 4000 rpm was used. Such spin-coating parameters typically resulted in an ultrathin film of approximately 40 nm in thickness, as demonstrated in the X-ray reflectivity measurement in Figure S1 in the Supporting Information. Spin-coated crystalline i-PHB films were then melted at 180 °C for 1 min followed by fast cooling down to room temperature before IRRAS measurements. After IRRAS examination, the samples were allowed for 10 day crystallization at room temperature before carrying out GIWAXD and POM studies. All measurements were carried out at room temperature.

Characterization. Infrared Reflection—Absorption Spectroscopy. A Thermo Nicolet 670 Nexus FT-IR spectrometer with a DTGS detector was used for IRRAS measurements. The IRRAS spectra were measured using a specular reflectance accessory (PIKE Tech. 80Spec) with a fixed incident angle of 80°. A blank AO substrate was used for background spectrum collection for polymers coated on an AO substrate. A PB substrate was used for background spectrum collection for polymers coated on a PB substrate. For a-PHB samples, all IR measurements were performed on the as-spin-coated films. Each spectrum was obtained by averaging 32 scans with 2 cm<sup>-1</sup> resolution from 600 to 4000 cm<sup>-1</sup>. The raw spectra were baseline-corrected using Essential FTIR software. All measurements were carried out at room temperature. IR peak decomposition (Gaussian fitting) was performed in GRAMS AI software. Fitting conditions of each spectrum will be discussed in subsequent sessions and fitting parameters are also shown in Table S1 in the Supporting Information.

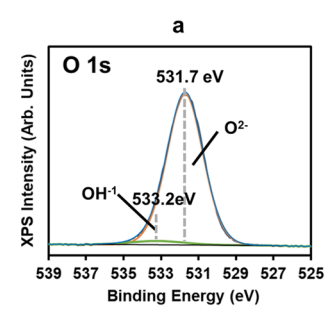
Grazing Angle X-ray Diffraction. A Xeuss 2.0 X-ray diffractometer was used for the study of crystallinity and crystallite orientation in i-PHB ultrathin films. The instrument was operated at a current of 0.6 mA and a voltage of 50 kV. Cu K- $\alpha$  radiation with an X-ray wavelength of 0.154 nm was used. The X-ray beam was aligned at a grazing angle of 0.2°, which is approximately 1.2 times the critical angle at the wavelength of 0.154. This grazing angle ensures that the X-ray beam penetrates the entire sample.

*X-ray Photoelectron Spectroscopy.* The X-ray photoelectron spectroscopy (XPS) profiles were measured using a Thermo Scientific K-A XPS instrument with an Al  $K\alpha$  X-ray source at an energy of 1486.6 eV and a base pressure below  $5 \times 10^{-8}$  Torr. A takeoff angle of 90° to the analyzer was used. A survey spectrum was collected with an energy range of 0–1200 eV (The survey spectrum is shown in the Supporting Information). The high-resolution spectra for C 1s, O 1s, and Al 2p were collected with a pass energy of 20 eV. Peak fitting was carried out using CasaXPS (version 2.3.16) software. All peak positions and relative sensitivity factors were calibrated to the C 1s peak at 285 eV. <sup>22</sup>

Polarized Optical Microscopy. In order to study the spherulitic morphology of i-PHB films after crystallization, an Olympus BX60 microscope equipped with a Nikon DS-Fi1 digital camera head and two cross polarizers was used. The image was recorded in the reflection mode.

## ■ RESULTS AND DISCUSSION

Figure 1a shows the XPS O 1s profiles for the aluminum substrate surface before boiling water treatment. The dominant peak is at 531.7 eV, indicating that the surface predominantly comprised AO. The small peak located at 533.2 eV, resolved by curve fitting, indicates the existence of a trace amount of OH<sup>-1</sup>. Figure 1b shows the O 1s profile after water treatment. The binding energies of the peaks after water treatment are consistent with those found for PB in the study by van den Brand *et al.*<sup>21</sup> Specifically, a strong peak at 531.9 eV indicates that a substantial amount of a new type of OH<sup>-1</sup> species was successfully introduced on the surface. In addition, the O<sup>2-</sup> peak was found shifting to 530.4 eV. This result indicates that a PB surface was formed after water treatment.



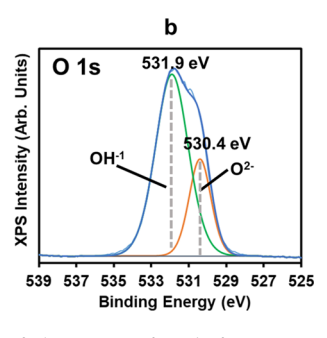


**Figure 1.** (a) XPS O 1s profiles of the AO surface before water treatment. (b) O 1s profiles of the AO sample surface after water treatment. Green and orange curves are for fitted peaks.

Intermolecular H-Bonding of a-PHB and PB. Initially, we will explore the intermolecular interaction between a-PHB and a PB surface. Because a-PHB is not able to crystallize, any observed infrared peak shift in the carbonyl region at a fixed temperature would, therefore, not be due to crystallization but due to the chemical interaction of the a-PHB with PB or, possibly, a confinement effect. Carbonyls restrained in a geometrically confined environment can have reduced mobility, possibly leading to a red shift of the IR peak. Therefore, it is important to decouple the confinement effect and other chemical effects. To eliminate the confinement effect, an a-PHB ultrathin film with the same thickness was also spin-coated on gold and AO substrates. Figure 2 shows the

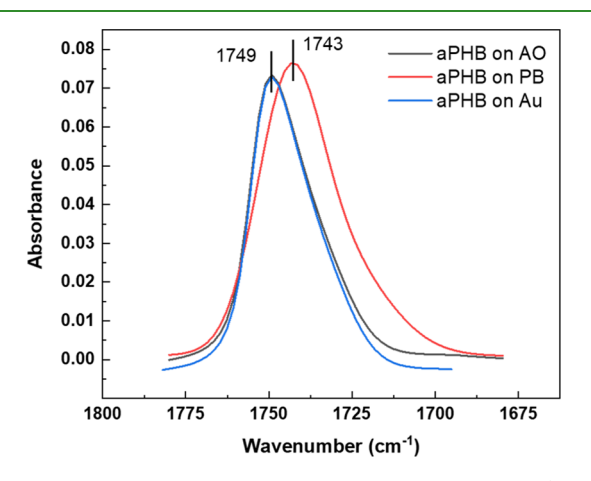
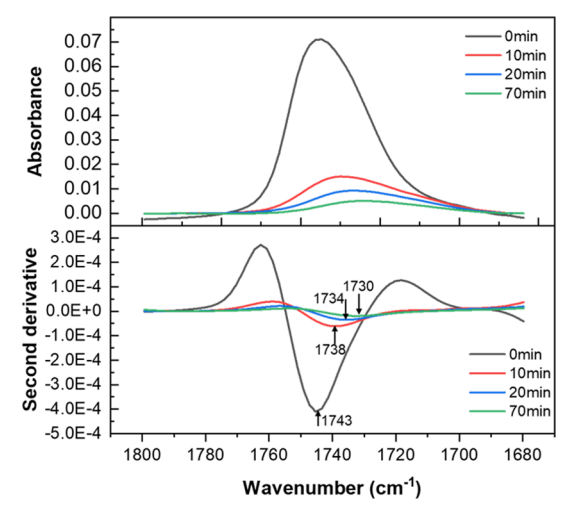


Figure 2. Carbonyl region of a-PHB ultrathin films on AO (black), PB (red), and gold (blue).

carbonyl region of the IRRAS spectra for a spin-coated a-PHB ultrathin film on AO, gold, and PB substrates measured at room temperature (23 °C). The a-PHB films on both gold and AO have a peak with its maximum located at 1749 cm<sup>-1</sup>, whereas a-PHB on PB has a peak at 1743 cm<sup>-1</sup>, indicating that a red shift only occurs for a-PHB/PB. If the red shift is induced by a geometric confinement effect, we should have observed a similar red shift for a-PHB on gold and AO. Thus, confinement should not be the reason for the red shift for the PB substrate. In addition, because a-PHB is not able to crystallize, the red shift should not be induced by crystallization but more likely associated with a chemical interaction between a-PHB and PB. Here, we hypothesize that the observed red shift for a-PHB on PB could arise from an intermolecular H-bonding interaction or, H-bond<sup>inter</sup>, formed between the -C=O of a-PHB and the surface -OH of PB.

To further understand the H-bond<sup>inter</sup>, it is important to obtain IRRAS spectra of the thin (several nanometers) layer in the interfacial region between the polymer and substrate. To achieve this goal, an immersion experiment was designed, wherein the as-cast film (40 nm in thickness) was immersed in a chloroform bath to let the solvent remove polymer from top layers. Because of the amorphous nature of a-PHB, it was assumed that once the solvent evaporates and enough relaxation time was given, structures of the as-spin-coated samples and chloroform-treated ones remain the same. The immersion experiment was carried out as a function of time and the sample was taken out at the time period of interest, dried completely, and equilibrated at room temperature at least for 6 h prior to the IRRAS measurement. Figure 3 shows the



**Figure 3.** Carbonyl region of a-PHB on PB with immersion times of 0, 10, 20, and 70 min and the corresponding second derivatives for each spectrum.

spectral changes in the carbonyl region at the immersion time of 10, 20, and 70 min. It was found that the carbonyl peak shifted from 1743 cm<sup>-1</sup> at 0 min down to 1730 cm<sup>-1</sup> at 70 min. The film thickness after each immersion step can be estimated based on the Beer-Lambert law, as shown in Table S2 in the Supporting Information. After 70 min, only an ultrathin layer of approximately 2.8 nm was left on the substrate. Therefore, from a thickness of 40 nm for the as-spincoated film to a 2.8 nm film, the carbonyl peak shifts from 1743 to 1730 cm<sup>-1</sup>, a 13 cm<sup>-1</sup> wavenumber shift. One may argue that such a prominent red shift could be due to a confinement effect induced by a decrease in the film thickness from 40 to 2.8 nm. To eliminate the possibility of confinement, IRRAS measurements were also carried out on a 1.4 nm a-PHB on an AO substrate, as shown in Figure S2 in the Supporting Information. The result shows that only a 2 cm<sup>-1</sup> red shift was observed for a-PHB on an AO substrate as the film thickness decreased from 40 to 1.4 nm. Therefore, the red shift observed in the current study for a-PHB on PB is not due to a confinement effect. Instead, the red shift is due to the Hbond<sup>inter</sup> predominately located in the interfacial region. As the film becomes thinner, the carbonyl band is composed more of the contribution from the H-bond component, leading to the overall carbonyl band red shift.

The 2.8 nm film of a-PHB on PB was then used to carry out peak decomposition to help extract the approximate absorption frequency of the H-bond<sup>inter</sup>. Specifically, a

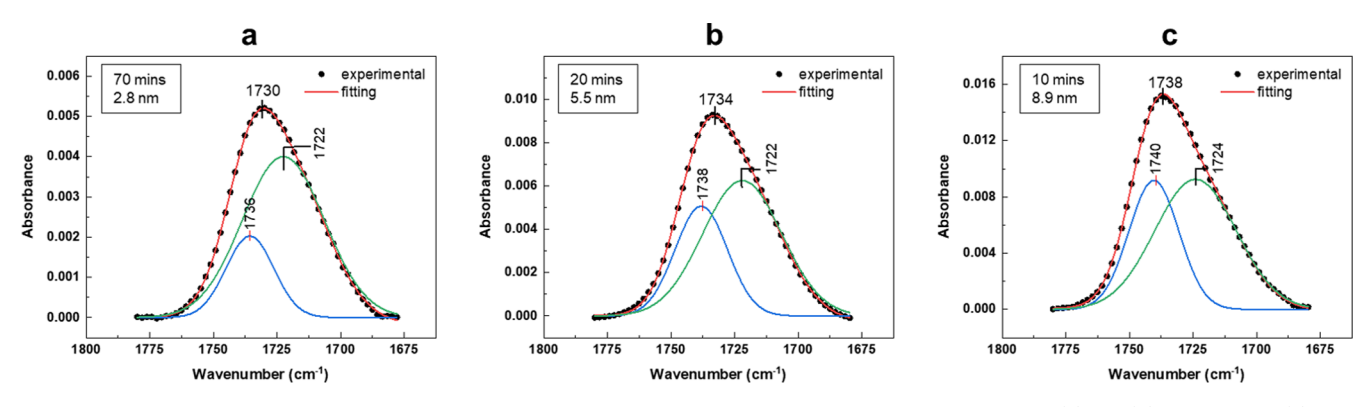


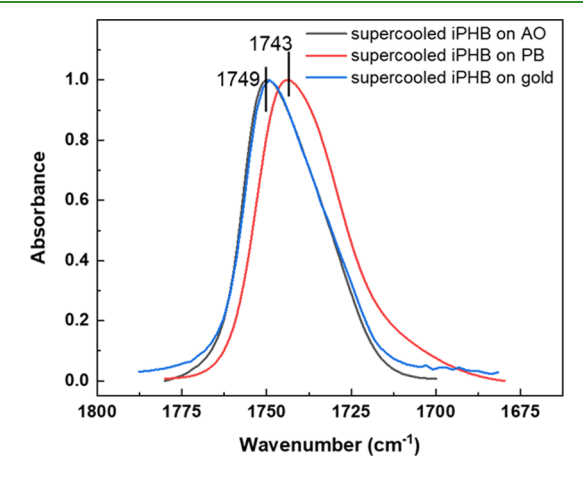
Figure 4. Peak decomposition for the carbonyl region of a-PHB ultrathin films on PB for immersion times of 70 (a), 20 (b), and 10 min (c). The corresponding film thickness is included in the left top in each plot.

Gaussian function was used to model the elemental peaks. At least two peaks are expected, including the undetermined Hbond inter peak and other peaks from amorphous carbonyls. The peak center for the amorphous peaks is not fixed. This is because the absorption frequency of amorphous carbonyls in PHB systems is highly sensitive to the local environment, manifested by slightly different frequencies identified in different PHB systems. <sup>23,24</sup> In addition, the H-bond<sup>inter</sup> may also shift the amorphous peak position. As a result, we found that a two-peak fitting gives the best convergence and the fitting result is shown in Figure 4a. The absorption frequency for the new H-bond<sup>inter</sup> formed between carbonyl from a-PHB and hydroxy from PB is determined to be approximately 1722 cm<sup>-1</sup>. The broadening of 1722 cm<sup>-1</sup> could result from the existence of a bonding energy distribution of the H bond between the oxygen from -C=O and hydrogen from Al-O-H. The 1736 cm<sup>-1</sup> is from the unbonded carbonyls in a more disordered state. It is noted that the 1736 cm<sup>-1</sup> frequency is lower than the typical "free" amorphous carbonyls of PHB in the bulk, which appear near 1740 cm<sup>-1</sup>.25,26 This 1736 cm<sup>-1</sup> peak indicates that those unbonded carbonyls are located in a somewhat constrained environment. PHB has been also found to form H-bond<sup>inter</sup> with other components, and a variety of peak frequencies for the H-bondinter have been reported. A Hbondinter at 1738 cm<sup>-1</sup> in the carbonyl region was found to be formed between -C=O of PHB and -OH of cellulose acetate butyrate. 17,25,27 PHB was also found to H-bond with catechin, having a H-bond<sup>inter</sup> at 1718.5 cm<sup>-1</sup>.<sup>28</sup> In the blend of PHB/ PVPh, the H-bond<sup>inter</sup> formed between -C=O of PHB and -OH of PVPh was at 1713 cm<sup>-1</sup>. 19,2

With the approximate peak position of the H-bond<sup>inter</sup> established, peak decompositions were then carried out for samples with immersion times of 20 and 10 min with the H-bond<sup>inter</sup> frequency fixed, as shown in Figure 4b,c. During fitting, for the 20 min (5.5 nm) sample, the peak center for H-bond<sup>inter</sup> is fixed at 1722 cm<sup>-1</sup> and for the 10 min (8.9 nm) sample, that for H-bond<sup>inter</sup> is fixed at 1724 cm<sup>-1</sup>. This is because 1724 cm<sup>-1</sup> provides a better fitting convergence and the difference between 1722 and 1724 cm<sup>-1</sup> is too small, given the spectral resolution of 2 cm<sup>-1</sup>. Fitting results show that the amorphous peak becomes more intense and shifts to a higher frequency, indicating that there is an increase in the fraction of carbonyls in a less restricted local environment with thicker

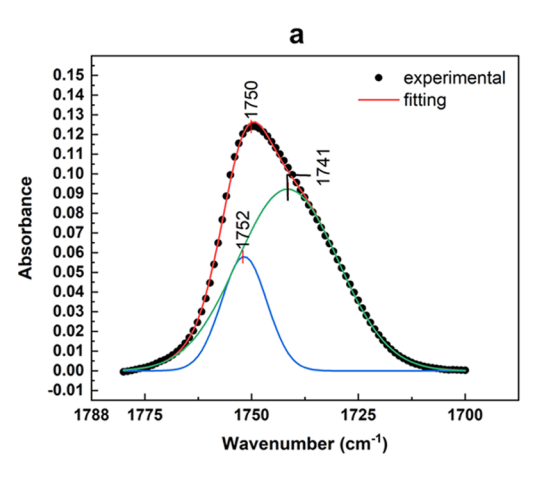
**Intermolecular H-Bonding of i-PHB with PB.** We now examine the intermolecular interaction of crystallizable i-PHB with PB. We will examine interactions of i-PHB with PB before

and after crystallization. In contrast to a-PHB, films made of i-PHB will crystallize during spin-coating because of their stereoregularity. Crystallization can occur during solvent evaporation during the spin-coating process. To remove the solvent effect on crystallization, after spin-coating, the sample was melted at 180 °C for 1 min and then allowed to contact a 5 °C copper block for 2 min to cool down. This was then followed by immediately recording the IRRAS spectrum at room temperature. Figure 5 shows the spectra taken right after



**Figure 5.** Carbonyl region for i-PHB ultrathin films on AO, PB, and gold measured at room temperature 2 min after melting. The spectra were scaled for visual comparison of peak shift. Raw spectra were shown in Figure S3 in the Supporting Information.

cooling for i-PHB on AO, PB, and gold. Because of the short time and rapid quench, i-PHB has not yet crystallized on the substrates. The peaks are very similar to that for a-PHB, as shown in Figure 2. That is, a red shift is observed only for i-PHB on PB in contrast to i-PHB on AO and gold, thus indicating the presence of the H-bond<sup>inter</sup> from i-PHB and PB. Peak decompositions for the AO and PB cases in Figure 5 are shown in Figure 6. For the fitting of i-PHB on AO, no peaks are fixed and two peaks at 1752 and 1741 cm<sup>-1</sup> can be resolved, indicating the presence of carbonyls in two different amorphous states. The 1741 cm<sup>-1</sup> band has been widely assigned as the typical "free" carbonyl in the bulk. 25 The 1752 cm<sup>-1</sup> peak implies carbonyls in an even more "free" local environment, which is likely from those in the free surface side, whereas the 1741 cm<sup>-1</sup> species is from regions beneath the free surface. Carbonyls with high frequencies beyond 1750 cm<sup>-1</sup>



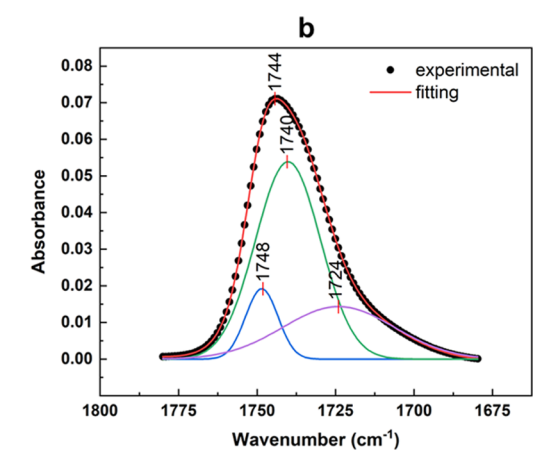


Figure 6. (a) Peak decomposition for the supercooled i-PHB film on AO. (b) Peak decomposition for the supercooled i-PHB film on PB.

were also reported in other studies. <sup>23,30</sup> For i-PHB on PB, the fitting was performed by fixing the peak center of H-bond<sup>inter</sup> at 1724 cm<sup>-1</sup> because of the existence of the H-bonding interaction. As a result, fitting gives additional two amorphous elements at 1748 and 1740 cm<sup>-1</sup>. Actually, this fitting gives a nearly zero residue, as shown in Table S2 in the Supporting Information, further confirming the existence of H-bond<sup>inter</sup> located at 1724 cm<sup>-1</sup> between i-PHB and PB.

Effects of PB on the Crystallization Behavior of i-PHB. The supercooled i-PHB films initially in the amorphous state eventually crystallize on both AO and PB substrates. After a 10 day period of crystallization at room temperature, IRRAS spectra, as shown in Figure 7, were taken on i-PHB on AO and

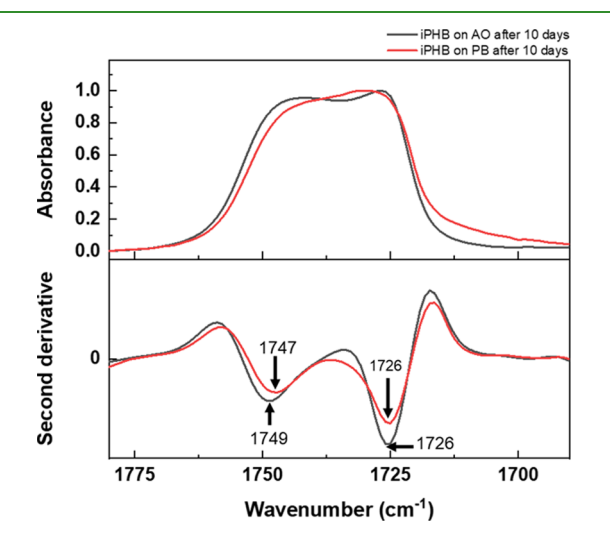


Figure 7. Carbonyl region for i-PHB ultrathin films on AO and PB substrates after a 10 day crystallization period at 23  $^{\circ}$ C and the corresponding second derivatives.

PB. Compared with spectra for i-PHB before crystallization in Figure 5, both samples have a peak at 1726 cm $^{-1}$ , which could be due to  $\alpha$  crystallization of i-PHB. After crystallization, the carbonyl regions for the two samples do not appear to be significantly different. Peak fittings for the spectra in Figure 7 were attempted. However, it was found that at least four elemental peaks were needed for the fit, and good convergence is not achieved. Other techniques may be needed to determine the buried elemental peaks.

To further confirm the development of  $\alpha$  crystals, GIWAXD measurements were carried out for i-PHB on gold, AO, and PB. As shown in Figure 8a, for i-PHB on gold, (020) diffraction peaks can be identified in both out-of-plane and inplane directions. The out-of-plane diffraction peak shows a stronger intensity indicating more crystals are in the edge-on orientation. In addition, two (020) peaks denoted by (020)<sub>H</sub> corresponding to smaller d-spacing and  $(020)_L$  corresponding to larger d-spacing can be identified. The  $(020)_{\rm H}$  peak most likely arises from more perfect crystals developed at high temperatures during cooling. Different (020) peaks for PHB thin films have also been observed in other studies.<sup>31</sup> This result implies that i-PHB tends to crystallize faster on the gold surface. For i-PHB on AO (Figure 8b), the diffraction peak intensity is still relatively strong but only diffraction from edgeon-oriented crystals can be observed. For i-PHB on PB (Figure 8c), the diffraction peak intensity is extremely weak with only a dim (020) diffraction ring observed. Such a low intensity with peak broadening indicates that for i-PHB on PB, crystals are less perfect and the crystallinity of the film is low. The ringshaped pattern indicates that the crystals are randomly oriented.

Film morphologies after crystallization were examined using POM, as shown in Figure 9. Two-dimensional spherulites can be clearly seen for the stereoregular i-PHB crystallized on gold and AO, whereas no spherulitic structure can be seen for i-

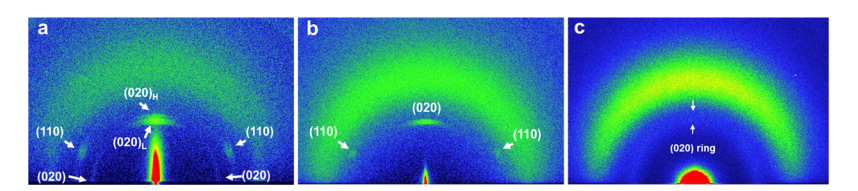


Figure 8. (a) GIWAXD profiles for i-PHB after a 10 day crystallization period at 23 °C on gold (a), AO (b), and PB (c), respectively. In graph c, two arrows were added to help identify the weak (020) diffraction ring. The broad peak at a high angle is from scattering from glass substrates.

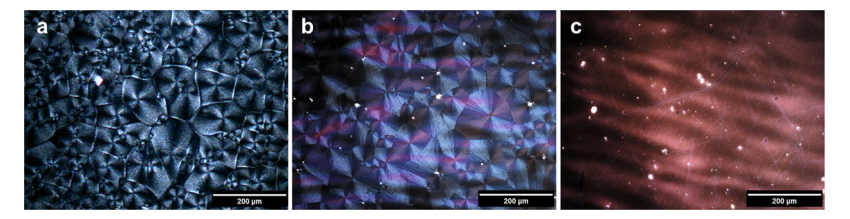


Figure 9. POM images of crystalline ultrathin films of i-PHB on Au (a), AO (b), and PB (c) substrates.

PHB crystallized on PB. However, given the occurrence of a weak (020) diffraction peak shown in GIWAXD data, some small crystallites developed in i-PHB ultrathin films on PB must still exist. Therefore, based on GIWAXD and POM results, a schematic is shown in Figure 10 to illustrate different

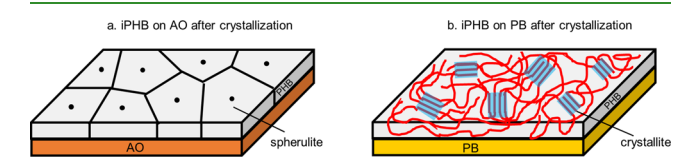


Figure 10. Representative schematics to illustrate hierarchical crystalline regions in i-PHB ultrathin films after crystallization on AO (a) and PB (b) substrates. The black dots in (a) represent nucleating spots. The red lines in (b) represent random coil chains and blue regions represent crystallites.

hierarchical crystal structures in the final as-crystallized films. For i-PHB on AO (Figure 10a), chains crystallize to form two-dimensional spherulites. During crystallization, chains have sufficient mobility to fold back and forth to form lamellar crystals and further assemble to form the hierarchical structure of spherulites. Crystals adopting the edge-on orientation facilitate the reduction of overall surface energy. In contrast, for i-PHB on PB (Figure 10b), because of the H-bonding interaction between PHB and PB, chain segmental mobility in the interfacial region is decreased and chains are prevented from freely forming chain-folded lamellae to further organize into spherulites. However, chain segments distant from the H-bonding region are less affected by the H-bonded interaction, enabling some crystallites to be formed near the free surface to give a fringed-micelle texture.

Although the IRRAS data shown in Figure 7 do not show much difference for crystalline i-PHB on AO and PB, GIWAXD and POM data do indicate that PB has a significant influence on i-PHB crystallization. Therefore, it is most likely that the IRRAS spectra shown in Figure 7 bear apparent similarity, whereas the elemental peak components could be very different. This possibility may be true especially considering the new H-bond<sup>inter</sup> between PHB and PB and the H-bond<sup>intra</sup> in the crystal of PHB exhibit a close absorption frequency. The carbonyl frequency due to H-bond<sup>intra</sup> is reported to occur at 1722 cm<sup>-1</sup>, which is very close to the frequency of the new H-bond<sup>inter</sup> found in the current study.

In addition, the relative stability of the H-bond<sup>inter</sup> can be qualitatively evaluated by comparing its formation enthalpy with the enthalpy of crystallization for stereoregular i-PHB  $\alpha$  crystals. The H-bonding enthalpy  $\Delta H^{AB}$  for polyesters (Lewis base) associated with a Lewis acid can be estimated using the relationship  $\Delta H^{AB} = -k^{AB}\Delta \nu^{AB}$ , where  $k^{AB} = 0.99$  kJ/mol and  $\Delta \nu^{AB}$  is the wavenumber shift of the carbonyl stretching mode from its amorphous state. <sup>32,33</sup> For the H-bond<sup>inter</sup> discussed in the current study, if the frequency of amorphous carbonyl for i-

PHB is taken as 1740 cm<sup>-1</sup>, then the H-bonding enthalpy is estimated to be 15.8 kJ/mol. This is higher than the  $\alpha$ crystallization enthalpy of i-PHB, which is 12.5 kJ/mol as reported by Sato et al.6 Bonding energy higher than the crystallization enthalpy is expected to alter nucleation mechanisms, slow down crystallization kinetics, and decrease crystallinity. Another possible factor that may influence the Hbond strength is the tacticity of the polymer. For example, in the PHB/PVPh study with related homo- and copolymers, it was also found that the intermolecular H-bonding enthalpy dropped from 23 to 21 kJ/mol in a-PHB and PHB, respectively.<sup>29</sup> However, in the present study, both a-PHB and i-PHB on PB show a similar magnitude in shift of the carbonyl stretching frequencies, suggesting that the tacticity itself may not influence the strength of the H bond much. This result is potentially due to the fact that PHB has a flexible chain and the H-bonding interaction between -C=O and -OH from PB is enough to obviate the tacticity effect.

#### CONCLUSIONS

In the present study, we have spun-coated a-PHB and i-PHB ultrathin films on PB flat surfaces and studied the interactions between PHB and PB. AO and gold substrates were used to eliminate the possibility of a confinement effect on crystallization. It was found that a-PHB can form H-bond<sup>inter</sup> with PB, as indicated by a new carbonyl peak located at approximately 1724 cm<sup>-1</sup>, suggesting a relatively strong Hbonded interaction. It was found that stereoregular i-PHB in the amorphous state was able to form similar H bonds with PB. Although i-PHB on PB eventually crystallizes, the preferred orientation of the crystals and the crystal morphologies are very different from those of i-PHB on AO. On an AO surface without H-bonded interactions, i-PHB crystals adopt an edgeon orientation and spherulites develop. On a PB surface with H-bonding interaction, small crystallites with random orientations are randomly distributed in the film near the free surface. The significant difference in crystallization behavior is related to the intermolecular H bond between PHB and PB. This study demonstrates a novel method of using PB to modulate the crystallization behavior of PHB thin films. The current findings could help design PHB/PB-based composite materials.

# ASSOCIATED CONTENT

## **Solution** Supporting Information

The Supporting Information is available free of charge at https://pubs.acs.org/doi/10.1021/acsapm.0c00758.

XRR data for a PHB film. Peak-fitting results of IRRAS spectra. Estimation method for film thickness based on IR peak intensity. Carbonyl peaks of a-PHB films of 1.4 nm *versus* 40 nm on AO. Raw IRRAS data for i-PHB on gold, AO, and PB (PDF)

# AUTHOR INFORMATION

#### **Corresponding Author**

John F. Rabolt — Department of Materials Science and Engineering, University of Delaware, Newark 19716, Delaware, United States; ⊚ orcid.org/0000-0003-4132-4266; Email: rabolt@udel.edu

#### **Authors**

- Changhao Liu Department of Materials Science and Engineering, University of Delaware, Newark 19716, Delaware, United States; Ocid.org/0000-0002-9103-8834
- Meng Jia Department of Chemistry, University of Delaware, Newark 19716, Delaware, United States; ⊚ orcid.org/0000-0002-8586-2384
- Jing Qu Advanced Materials Characterization Lab, University of Delaware, Newark 19716, Delaware, United States
- Isao Noda Department of Materials Science and Engineering, University of Delaware, Newark 19716, Delaware, United States; Danimer Scientific, Bainbridge 39817, Georgia, United States
- D. Bruce Chase Department of Materials Science and Engineering, University of Delaware, Newark 19716, Delaware, United States
- Reva Street Department of Materials Science and Engineering, University of Delaware, Newark 19716, Delaware, United States

Complete contact information is available at: https://pubs.acs.org/10.1021/acsapm.0c00758

#### Notes

The authors declare no competing financial interest.

#### ACKNOWLEDGMENTS

This publication was made possible by the National Science Foundation (NSF) Delaware EPSCoR grant nos. 1301765 and 1757353 and the State of Delaware. The authors would also like to acknowledge support from the NSF DMR Polymers Program Grant DMR 1407255.

# REFERENCES

- (1) Anderson, A. J.; Dawes, E. A. Occurrence, Metabolism, Metabolic Role, and Industrial Uses of Bacterial Polyhydroxyalkanoates. *Microbiol. Mol. Biol. Rev.* **1990**, *54*, 450–472.
- (2) Iwata, T.; Doi, Y. Crystal Structure and Biodegradation of Aliphatic Polyester Crystals. *Macromol. Chem. Phys.* **1999**, 200, 2429—2442.
- (3) Yokouchi, M.; Chatani, Y.; Tadokoro, H.; Teranishi, K.; Tani, H. Structural studies of polyesters: 5. Molecular and crystal structures of optically active and racemic poly ( $\beta$ -hydroxybutyrate). *Polymer* **1973**, 14, 267–272.
- (4) Philip, S.; Keshavarz, T.; Roy, I. Polyhydroxyalkanoates: Biodegradable Polymers with a Range of Applications. *J. Chem. Technol. Biotechnol.* **2007**, 82, 233–247.
- (5) Liu, C.; Noda, I.; Martin, D. C.; Chase, D. B.; Ni, C.; Rabolt, J. F. Growth of anisotropic single crystals of a random copolymer, poly[(R)-3-hydroxybutyrate-co-(R)-3-hydroxyhexanoate] driven by cooperative -CH···O H-bonding. *Polymer* **2018**, *154*, 111–118.
- (6) Sato, H.; Murakami, R.; Padermshoke, A.; Hirose, F.; Senda, K.; Noda, I.; Ozaki, Y. Infrared Spectroscopy Studies of CH···O Hydrogen Bondings and Thermal Behavior of Biodegradable Poly(hydroxyalkanoate). *Macromolecules* **2004**, *37*, 7203–7213.
- (7) Dai, X.; Zhang, J.; Ren, Z.; Li, H.; Sun, X.; Yan, S. A Grazing Incident XRD Study on the Structure of Poly(3-Hydroxybutyrate) Ultrathin Films Sandwiched between Si Wafers and Amorphous Polymers. *Polym. Chem.* **2016**, *7*, 3705–3713.

- (8) Napolitano, S.; Wübbenhorst, M. Slowing Down of the Crystallization Kinetics in Ultrathin Polymer Films: A Size or an Interface Effect? *Macromolecules* **2006**, *39*, 5967–5970.
- (9) Khasanah; Reddy, K. R.; Ogawa, S.; Sato, H.; Takahashi, I.; Ozaki, Y. Evolution of Intermediate and Highly Ordered Crystalline States under Spatial Confinement in Poly(3-Hydroxybutyrate) Ultrathin Films. *Macromolecules* **2016**, *49*, 4202–4210.
- (10) Sun, X.; Chen, Z.; Wang, F.; Yan, S.; Takahashi, I. Influence of Poly(Vinylphenol) Sublayer on the Crystallization Behavior of Poly(3-Hydroxybutyrate) Thin Films. *Macromolecules* **2013**, 46, 1573—1581
- (11) Sun, X.; Gao, N.; Li, Q.; Zhang, J.; Yang, X.; Ren, Z.; Yan, S. Crystal Morphology of Poly(3-Hydroxybutyrate) on Amorphous Poly(Vinylphenol) Substrate. *Langmuir* **2016**, 32, 3983–3994.
- (12) Zhou, J.; Gan, H.; Ren, Z.; Li, H.; Zhang, J.; Sun, X.; Yan, S. The Effect of Poly(Vinyl Phenol) Sublayer on the Crystallization and Melting Behavior of Poly(3-Hydroxybutyrate) via Hydrogen Bonds. *Polymer* **2014**, *55*, 5821–5828.
- (13) Yan, C.-z.; Guo, L.; Sun, X.-l.; Yan, S.-k.; Takahashi, I. Temperature-Driven Surface Morphology Evolution of Poly(3-Hydroxybutyrate) Single Layer and Poly(3-Hydroxybutyrate)/Poly-(Vinyl Phenol) Bilayer on Si Wafers. *Chin. J. Polym. Sci.* **2013**, *31*, 407–418.
- (14) Liu, C.; Noda, I.; Chase, D. B.; Zhang, Y.; Qu, J.; Jia, M.; Ni, C.; Rabolt, J. F. Crystallization Retardation of Ultrathin Films of Poly[(R)-3-Hydroxybutyrate] and a Random Copolymer Poly[(R)-3-Hydroxybutyrate-Co-(R)-3-Hydroxyhexanoate] on an Aluminum Oxide Surface. *Macromolecules* **2019**, *52*, 7343–7352.
- (15) van den Brand, J.; Blajiev, O.; Beentjes, P. C. J.; Terryn, H.; de Wit, J. H. W. Interaction of Ester Functional Groups with Aluminum Oxide Surfaces Studied Using Infrared Reflection Absorption Spectroscopy. *Langmuir* **2004**, *20*, 6318–6326.
- (16) Liascukiene, I.; Aissaoui, N.; Asadauskas, S. J.; Landoulsi, J.; Lambert, J.-F. Ordered Nanostructures on a Hydroxylated Aluminum Surface through the Self-Assembly of Fatty Acids. *Langmuir* **2012**, *28*, 5116–5124.
- (17) Suttiwijitpukdee, N.; Sato, H.; Unger, M.; Ozaki, Y. Effects of Hydrogen Bond Intermolecular Interactions on the Crystal Spherulite of Poly(3-Hydroxybutyrate) and Cellulose Acetate Butyrate Blends: Studied by FT-IR and FT-NIR Imaging Spectroscopy. *Macromolecules* **2012**, *45*, 2738–2748.
- (18) Lim, J. S.; Noda, I.; Im, S. S. Effect of Hydrogen Bonding on the Crystallization Behavior of Poly(3-Hydroxybutyrate-Co-3-Hydroxyhexanoate)/Silica Hybrid Composites. *Polymer* **2007**, *48*, 2745—2754
- (19) Guo, L.; Sato, H.; Hashimoto, T.; Ozaki, Y. FTIR Study on Hydrogen-Bonding Interactions in Biodegradable Polymer Blends of Poly(3-Hydroxybutyrate) and Poly(4-Vinylphenol). *Macromolecules* **2010**, *43*, 3897–3902.
- (20) Yu, H.-Y.; Yao, J.-M. Reinforcing Properties of Bacterial Polyester with Different Cellulose Nanocrystals via Modulating Hydrogen Bonds. *Compos. Sci. Technol.* **2016**, *136*, 53–60.
- (21) van den Brand, J.; Sloof, W. G.; Terryn, H.; de Wit, J. H. W. Correlation between Hydroxyl Fraction and O/Al Atomic Ratio as Determined from XPS Spectra of Aluminium Oxide Layers. *Surf. Interface Anal.* **2004**, *36*, 81–88.
- (22) Moulder, J. F. Handbook of X-Ray Photoelectron Spectroscopy; Physical Electronics, 1995; pp 230–232.
- (23) Chen, Y.; Park, Y.; Noda, I.; Jung, Y. M. Influence of Polyethylene Glycol (PEG) Chain Length on the Thermal Behavior of Spin-Coated Thin Films of Biodegradable Poly(3-Hydroxybutyrate-Co-3-Hydroxyhexanoate)/PEG Blends. J. Mol. Struct. 2016, 1124, 159–163.
- (24) Chen, Y.; Noda, I.; Jung, Y. M. Revealing thermal behavior of poly(3-hydroxybutyrate- co -3-hydroxyhexanoate) and its polyethylene glycol blends thin films: Effect of 3-Hydroxyhexanoate comonomer content. *J. Mol. Struct.* **2018**, *1162*, 140–144.
- (25) Suttiwijitpukdee, N.; Sato, H.; Zhang, J.; Hashimoto, T. Effects of Intermolecular Hydrogen Bondings on Isothermal Crystallization

- Behavior of Polymer Blends of Cellulose Acetate Butyrate and Poly(3-Hydroxybutyrate). *Macromolecules* **2011**, *44*, 3467–3477.
- (26) Sobieski, B. J.; Noda, I.; Rabolt, J. F.; Chase, D. B. Observation of Intermolecular Hydrogen Bonding Interactions in Biosynthesized and Biodegradable Poly [(R)-3-hydroxybutyrate-co-(R)-3-hydroxyhexanoate] in Chloroform and 1,1,1,3,3,3-Hexafluoro-2-propanol (HFIP). *Appl. Spectrosc.* **2017**, *71*, 2339–2343.
- (27) Suttiwijitpukdee, N.; Sato, H.; Zhang, J.; Hashimoto, T.; Ozaki, Y. Intermolecular Interactions and Crystallization Behaviors of Biodegradable Polymer Blends between Poly (3-Hydroxybutyrate) and Cellulose Acetate Butyrate Studied by DSC, FT-IR, and WAXD. *Polymer* 2011, 52, 461–471.
- (28) Zhu, B.; Li, J.; He, Y.; Osanai, Y.; Matsumura, S.; Inoue, Y. Thermal and Infrared Spectroscopic Studies on Hydrogen-Bonding Interaction of Biodegradable Poly(3-Hydroxybutyrate)s with Natural Polyphenol Catechin. *Green Chem.* **2003**, *5*, 580–586.
- (29) Iriondo, P.; Iruin, J. J.; Fernandez-Berridi, M. J. Association Equilibria and Miscibility Prediction in Blends of Poly(vinylphenol) with Poly(hydroxybutyrate) and Related Homo- and Copolymers: An FTIR Study. *Macromolecules* 1996, 29, 5605–5610.
- (30) Chen, Y.; Noda, I.; Jung, Y. M. Revealing thermal behavior of poly(3-hydroxybutyrate- co -3-hydroxyhexanoate) and its polyethylene glycol blends thin films: Effect of 3-Hydroxyhexanoate comonomer content. *J. Mol. Struct.* **2018**, *1162*, 140–144.
- (31) Khasanah; Reddy, K. R.; Ogawa, S.; Sato, H.; Takahashi, I.; Ozaki, Y. Evolution of Intermediate and Highly Ordered Crystalline States under Spatial Confinement in Poly(3-Hydroxybutyrate) Ultrathin Films. *Macromolecules* **2016**, *49*, 4202–4210.
- (32) Fowkes, F. M.; Tischler, D. O.; Wolfe, J. A.; Lannigan, L. A.; Ademu-John, C. M.; Halliwell, M. J. Acid-base complexes of polymers. *J. Polym. Sci., Polym. Chem. Ed.* **1984**, 22, 547–566.
- (33) Brogly, M.; Grohens, Y.; Labbe, C.; Schultz, J. Influence of Tacticity on the Conformation and Development of Acid-Base Adducts of PMMA Homopolymers Adsorbed on Aluminium Mirrors. *Int. J. Adhes. Adhes.* 1997, 17, 257–261.